Interferon Regulatory Factors IRF5 and IRF7 Inhibit Growth and Induce Senescence in Immortal Li-Fraumeni Fibroblasts

Qunfang Li,[1] Lin Tang,[1] Paul Christopher Roberts,[2] Janice M. Kraniak,[1] Aviva Levine Fridman,[1] Olga I. Kulaeva,[1] Omid S. Tehrani,[1] and Michael A. Tainsky[1,3]

[1]Program in Molecular Biology and Genetics, Barbara Ann Karmanos Cancer Institute, [2]Department of Immunology and Microbiology, and [3]Center for Molecular Medicine and Genetics, Wayne State University School of Medicine, Detroit, Michigan

Abstract

Cellular immortalization is one of the prerequisite steps in carcinogenesis. By gene expression profiling, we have found that genes in the interferon (IFN) pathway were dysregulated during the spontaneous cellular immortalization of fibroblasts from Li-Fraumeni syndrome (LFS) patients with germ-line mutations in *p53*. IFN signaling pathway genes were down-regulated by epigenetic silencing during immortalization, and some of these same IFN-regulated genes were activated during replicative senescence. Bisulfite sequencing of the promoter regions of two IFN regulatory transcription factors (*IRF5* and *IRF7*) revealed that *IRF7*, but not *IRF5*, was epigenetically silenced by methylation of CpG islands in immortal LFS cells. The induction of *IRF7* gene by IFNα in immortal LFS cells was potentiated by pretreatment with the demethylation agent 5-aza-2′-deoxycytidine. Overexpression of IRF5 and IRF7 revealed that they can act either alone or in tandem to activate other IFN-regulated genes. In addition, they serve to inhibit the proliferation rate and induce a senescence-related phenotype in immortal LFS cells. Furthermore, polyinosinic:polycytidylic acid treatment of the IRF-overexpressing cells showed a more rapid induction of several IFN-regulated genes. We conclude that the epigenetic inactivation of the IFN pathway plays a critical role in cellular immortalization, and the reactivation of IFN-regulated genes by transcription factors IRF5 and/or IRF7 is sufficient to induce cellular senescence. The IFN pathway may provide valuable molecular targets for therapeutic interventions at early stages of cancer development. (Mol Cancer Res 2008;6(5):770–84)

Introduction

Normal mammalian somatic cells have a limited life span *in vitro* called the "Hayflick limit" (1), in which cells exit the cell cycle and undergo a series of biochemical and morphologic changes resulting in cellular senescence (2). Cellular immortalization is one of the prerequisite steps in carcinogenesis, which can be defined as an acquired capacity of normal cells to escape replicative senescence and to grow indefinitely. However, immortality is reversible and senescence-like growth arrest can be restored by induction of genes including *p53, p63, p73, RB, p21^{CIP1}, p16^{INK4a}, p15^{INK4B}, p57^{KIP2}, E2, IGFBP-rP1, RAF-1*, and mitogen-activated protein kinase kinase *MKK6* (3).

Li-Fraumeni syndrome (LFS) is a rare familial dominant inherited cancer syndrome typified by early onset of cancer and multiple cancer types in which 75% of the LFS patients carry a germ-line mutation in one allele of the *p53* gene (4-6). Fibroblasts from LFS patients spontaneously immortalize in culture and there is a high frequency of somatic mutation in the remaining wild-type allele of *p53* in those immortal cells (7, 8). In addition to loss of *p53*, alterations such as stabilization of telomere length, multiple chromosomal aberrations, and epigenetic promoter silencing are necessary for the induction of cellular immortalization (9). Using four independent spontaneously immortalized LFS cell lines [MDAH041 (telomerase positive) and three MDAH087 cell lines, MDAH087-N, MDAH087-1, and MDAH087-10 (telomerase negative)] from two LFS patients (7, 8), we conducted a systematic analysis of the gene expression changes acquired during immortalization and found that the interferon (IFN) pathway, cell cycle genes, and cytoskeletal genes were dysregulated during the immortalization process (7, 10, 11).

DNA methylation, an epigenetic modification in CpG islands, results in transcriptional silencing of the genes that can alter genomic imprinting (12), chromatin structure modulation (13), development (14), somatic X-chromosome inactivation, and suppression of transposable elements (15). The 5-methylcytosine content of DNA markedly decreases in aging normal diploid fibroblasts, whereas methylation of DNA is stable in immortal cells (16). About 60% of mammalian

Received 3/6/07; revised 12/12/07; accepted 2/7/08.
Grant support: Barbara and Fred Erb Endowed Chair in Cancer Genetics (M.A. Tainsky), the Karmanos Cancer Institute, the State of Michigan Life Sciences Corridor, the Molecular Medicine and Genetics Applied Genomics Technology Center at Wayne State University, and the Genomics and Biostatistics Cores of the Karmanos Cancer Institute, grant P30CA022453.
The costs of publication of this article were defrayed in part by the payment of page charges. This article must therefore be hereby marked *advertisement* in accordance with 18 U.S.C. Section 1734 solely to indicate this fact.
Note: Supplementary data for this article are available at Molecular Cancer Research Online (http://mcr.aacrjournals.org/).
Current address for P.C. Roberts: Department of Biomedical Sciences and Pathobiology, Virginia Tech. University, Blacksburg, VA 24061.
Requests for reprints: Michael A. Tainsky, Program in Molecular Biology and Genetics, Barbara Ann Karmanos Cancer Institute, Wayne State University School of Medicine, 110 East Warren, Detroit, MI 48201. Phone: 313-578-4340; Fax: 313-832-7294. E-mail: tainskym@karmanos.org

doi:10.1158/1541-7786.MCR-07-0114

genes have CpG islands in their promoter regions, which, under normal circumstances, are not methylated. In tumor cells, hypermethylation of the CpG islands in promoters results in transcriptional inhibition of tumor suppressor genes (17-19). Abnormal promoter hypermethylation and subsequent silencing of gene expression of $p16^{INK4a}$, $p15^{INK4B}$, $p14^{ARF}$, *p73, APC*, and *BRCA1* has revealed that epigenetic changes are one of the common mechanisms leading to cancer (20, 21). 5-Aza-2′-deoxycytidine (5-aza-dC), a cytosine analogue and a DNA methyltransferase inhibitor, has been used to study epigenetic silencing of key regulatory genes in cancer and to induce senescence in immortal cells (22-24). Treatment with 5-aza-dC leads to DNA hypomethylation, which results in reactivation of epigenetically silenced genes (24-26).

Previously, we found that the IFN signaling pathway was disrupted during cellular immortalization of all four immortal LFS cell lines through methylation-dependent gene silencing (26). The IFN signaling pathway may be a tumor-suppressive pathway, and thus dysregulation of this pathway might play a critical role in cellular immortalization. As part of the innate immune response, type I IFNs (IFNα, IFNβ, and IFNω) play essential roles in protecting cells from viral infection and exhibit antiproliferative and immunomodulatory activities (27, 28). Type I IFNs elicit their biological functions through the transcriptional activation of target genes by the Janus-activated kinase/signal transducer and activator of transcription (STAT) signaling pathway and the family of IFN regulatory transcription factors (IRF; refs. 28-30). These transcription factors up-regulate certain immediate-early genes such as *IFNα4* and *IFNβ*. These early response IFNs, in an autocrine or paracrine manner, lead to the expression of IFN regulatory factor 7 (*IRF7*) and other secondary antiviral response genes (29, 31).

The IRFs belong to a growing family of transcription factors with a broad range of activities. IRF7 is an IFN-inducible transcription factor necessary for IFN-stimulated gene (ISG) induction by IFNs (29, 31, 32). When activated by phosphorylation, IRF7 translocates from the cytoplasm to the nucleus to induce target gene expression by binding to promoter regulatory elements (33, 34). IRF7 is not normally expressed in cells, but can be induced by IFNα, the STAT pathway, double-stranded RNA, or viral infection. Together with IRF3 and IRF5, IRF7 regulates the late wave (or phase) of transcription of IFN-regulated genes after viral infection. The lack of IRF7 expression in 2fTGH fibrosarcoma cells and several lung cancer cell lines correlated with CpG island hypermethylation in its promoter region and indicated that epigenetic promoter silencing of the *IRF7* gene does occur in cancer cells (35, 36). Similarly, we also found that *IRF7* was down-regulated in preneoplastic immortal cells, and its expression could be restored by DNA demethylation (26). Another IFN regulatory factor, IRF5, has a similar function in the induction of type I IFN genes. However, the phosphorylation of IRF5 is virus specific and induces *IFNα8* genes (37). IRF5 can also induce G_2-M growth arrest and apoptosis by modulating gene expression in a *p53*-independent manner. Consistent with cell cycle regulatory role, loss of IRF5 expression was observed in many primary hematologic malignancies (38). Several IRF family members including IRF1 and IRF3 have been shown to regulate tumor suppressor genes and induce growth arrest and/or apoptosis (39-42). Thus, the IFN signaling pathway and IRFs may provide promising new targets for cancer treatment.

In this report, we have focused on elucidating the mechanism(s) responsible for repression of the IFN signaling pathway during immortalization and identifying the responsible transcriptional regulators. Although all LFS cells exhibited a decrease in ISG expression, demethylation agent 5-aza-dC could reactivate IFN-regulated gene expression in those immortal LFS cells. Bisulfite sequencing of the promoter regions of two IFN regulatory transcription factors (*IRF5* and *IRF7*) revealed that *IRF7*, but not *IRF5*, was epigenetically silenced by methylation of CpG islands in immortal LFS cells. Overexpression of IRF5 and/or IRF7 in immortal LFS cells, alone or in combination, resulted in (*a*) up-regulation of other ISGs, (*b*) a faster and stronger IFN induction on polyinosinic:polycytidylic acid (polyI:C) treatment, (*c*) inhibition of cell growth, and (*d*) induction of a senescence-like phenotype in two independent immortal LFS cells. We conclude that the disruption of proper IFN signaling plays a functional role in cellular immortalization, and activation of IFN-regulated genes through transcription factors IRF5 and/or IRF7 is capable of inducing senescence.

Results

IFN-Stimulated Genes Are Differentially Regulated in Immortal and Senescent LFS Fibroblast Cells

Using gene expression profiling analysis, we have previously found that spontaneous immortalization of LFS cell lines correlated with epigenetic gene silencing due to promoter CpG methylation (26). We identified a number of genes whose expression level was down-regulated after immortalization but up-regulated by 5-aza-dC treatment, suggesting that these genes may be epigenetically regulated by promoter hypermethylation during immortalization. Among these genes, we found a significant number of ISGs as well as other genes involved in the IFN signaling pathways. Because the IFN signaling pathway is a growth-suppressive pathway, we hypothesized that its impairment might represent an important early event in carcinogenesis, specifically associated with immortalization. Further analysis of the ISGs differentially expressed among the four immortal LFS cell lines using hierarchical clustering (Supplementary Fig. S1A) and multidimensional scaling analysis (Supplementary Fig. S1B) supported the previous observations that treatment of immortal cell lines with 5-aza-dC could reverse immortality and induce senescence (10, 24, 43). Both methods confirmed the dysregulation of distinct sets of ISGs within the LFS cell lines studied, indicating that the mechanisms involved in the disruption of the IFN pathway might differ from cell line to cell line but that the IFN pathway was consistently abrogated.

We examined the expression of a representative set of ISGs using quantitative reverse transcription-PCR (RT-PCR) to confirm the gene expression changes found in our microarray data. *TLR3, IFNα, IFNβ, IRF5, IRF7, STAT1*, and *OAS1* were selected from those genes that were up-regulated following 5-aza-dC treatment (10, 43), as well as transcription factors and genes downstream in the IFN pathway. The quantitative RT-PCR results of untreated, immortalized cells showed

down-regulation of these ISGs albeit to different extents in each of the four immortal cell lines as compared with the isogenic precrisis LFS cells (Table 1A). Consistent with microarray findings, the expressions of these genes were all induced following 5-aza-dC treatment (Table 1B). Western blot analysis of selected ISGs revealed similar results (data not shown and refs. 10, 43). PolyI:C treatment, which mimics viral infection and induces the IFN pathway, failed to induce IFN-regulated gene activation in three of four immortal LFS cell lines, also indicating a functional inactivation of this pathway (data not shown). Thus, these results confirmed the disruption of the IFN pathway through epigenetic silencing during immortalization of all four LFS cell lines.

Immortalization of LFS fibroblasts, which occurs at low frequency in culture, results from cells escaping from senescence. We sought to determine whether up-regulation of IFN-regulated genes was associated with cellular senescence. Precrisis MDAH041 were grown in culture to 23 population doublings (PD 23), at which point senescence-associated β-galactosidase (β-gal) assay indicated that 40% to 60% of the these cells had entered into senescence (data not shown). Quantitative RT-PCR was then used to compare ISG mRNA expression of these senescent cells (PD 23) to proliferating early PD (PD 13) MDAH041 cells. We found that expression of four of six IFN-regulated genes had increased by at least 3-fold at senescence, with the most significant change in *IFNα* (Table 2). Quantitative RT-PCR done on senescing normal HCA2 (PD 75) and AFB-10 (PD 21) fibroblasts gave similar results with even more significant induction of ISGs (Table 2) when they were compared with normal proliferating AFB-10 fibroblasts (PD 1). By Western blot analysis of senescing MDAH041 cells (PD 23), we observed increased expression of IRF5, IRF7, and STAT1 proteins during senescence, as well as an increase in STAT1 phosphorylation at Tyr^{701} (Fig. 1). The induction of these genes in senescing cells strongly supported that the IFN pathway is a growth-suppressive pathway (44-48) and its repression is a requirement for immortalization.

Table 1. Quantitative RT-PCR Analysis of ISG Expression in LFS Fibroblast Cells

(A) Immortal vs Precrisis Cells

	MDAH041	MDAH087-N	MDA087-1	MDAH087-10
TLR3	−16.34	−1.62	−1.53	−2.87
IFNα	−40.79	2.08	−9.65	−3.12
IFNβ	−4.08	2.01	−30.7	−26.35
IRF7	−147.03	−6.63	−48.5	−139.1
IRF5	−176.07	−7.36	−1.69	−3.25
STAT1	−14.32	−7.73	−8.46	−288.01
OAS1	−8.4	−11.96	−33.82	−39.12

(B) 5-Aza-dC–Treated vs Untreated Immortal Cells

	MDAH041	MDAH087-N	MDA087-1	MDAH087-10
TLR3	2.68	2.64	2.33	1.68
IFNα	−1.26	1.22	1.36	−1.13
IFNβ	6.63	4.96	22.16	3.76
IRF7	421.68	12.65	3.51	4.92
IRF5	9.38	2.38	3.43	2.22
STAT1	119.85	9.05	1.56	3.23
OAS1	64.45	8.37	2.99	5.66

NOTE: Fold changes in expression of seven ISGs were calculated by quantitative RT-PCR after immortalization (A) and after treatment with 5-aza-dC (B).

Table 2. Quantitative RT-PCR Analysis of ISG Expression in Senescing MDAH041 and Normal Fibroblast Cells Compared with Early PD Cells

	MDAH041	HCA2	AFB-10
TLR3	−1.24	7.89	16.91
IFNα	93.05	−1.54	11.47
IFNβ	8.46	3.61	25.99
IRF5	9.58	5.98	4.17
IRF7	3.43	82.14	25.99
STAT1α	−1.64	56.49	30.06

NOTE: Expression levels of six ISGs in senescing MDAH041 cells (PD 23) were compared with early PD, nonsenescing MDAH041 cells (PD 13) by quantitative RT-PCR. Quantitative RT-PCR of those six ISGs was also done on senescing normal human fibroblasts HCA2 (PD 75) and AFB-10 cells (PD 21), whereas AFB-10 (PD 1) was used as nonsenescing normal control fibroblasts.

Promoter Methylation Analysis of Normal and LFS Fibroblast Cells

We have observed that the repressed *IRF5* and *IRF7* genes could be reactivated on demethylation treatment (Table 1B). To investigate whether the genes for these two critical IFN regulatory factors were silenced by promoter hypermethylation, we examined 1,000 bp upstream and downstream to the transcription start site of these genes and identified CpG islands using MethPrimer software (49). Within a 2,000-bp region around each transcription start site, large computational CpG islands were found in the promoter regions of both genes (−415 to +197 bp for *IRF5* and −280 to +324 for *IRF7*). To determine the methylation status of the CpG islands in these two genes, we carried out PCR and DNA sequencing of these regions using sodium bisulfite–modified genomic DNA from normal and LFS cells. Interestingly, we found that the *IRF7* gene was heavily methylated (>97% of the total 31 CpG dinucleotides) in the promoter region of immortal MDAH041 cells, partially methylated in the precrisis cells, and not methylated (<2%) in

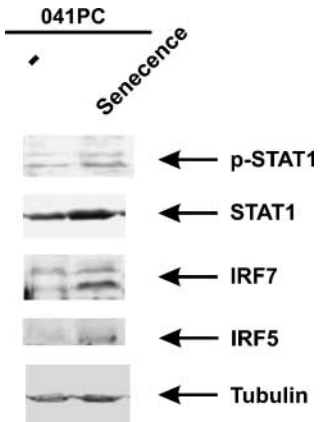

FIGURE 1. Western blot of 041PC senescent cells. Western blots for phospho-STAT1 (Tyr^{701}; *p-STAT1*), STAT1, IRF7, and IRF5 were done on senescing MDAH041 cells compared with early nonsenescing cells (p13). Tubulin was used as a loading control. 041PC, MDAH041 precrisis cells.

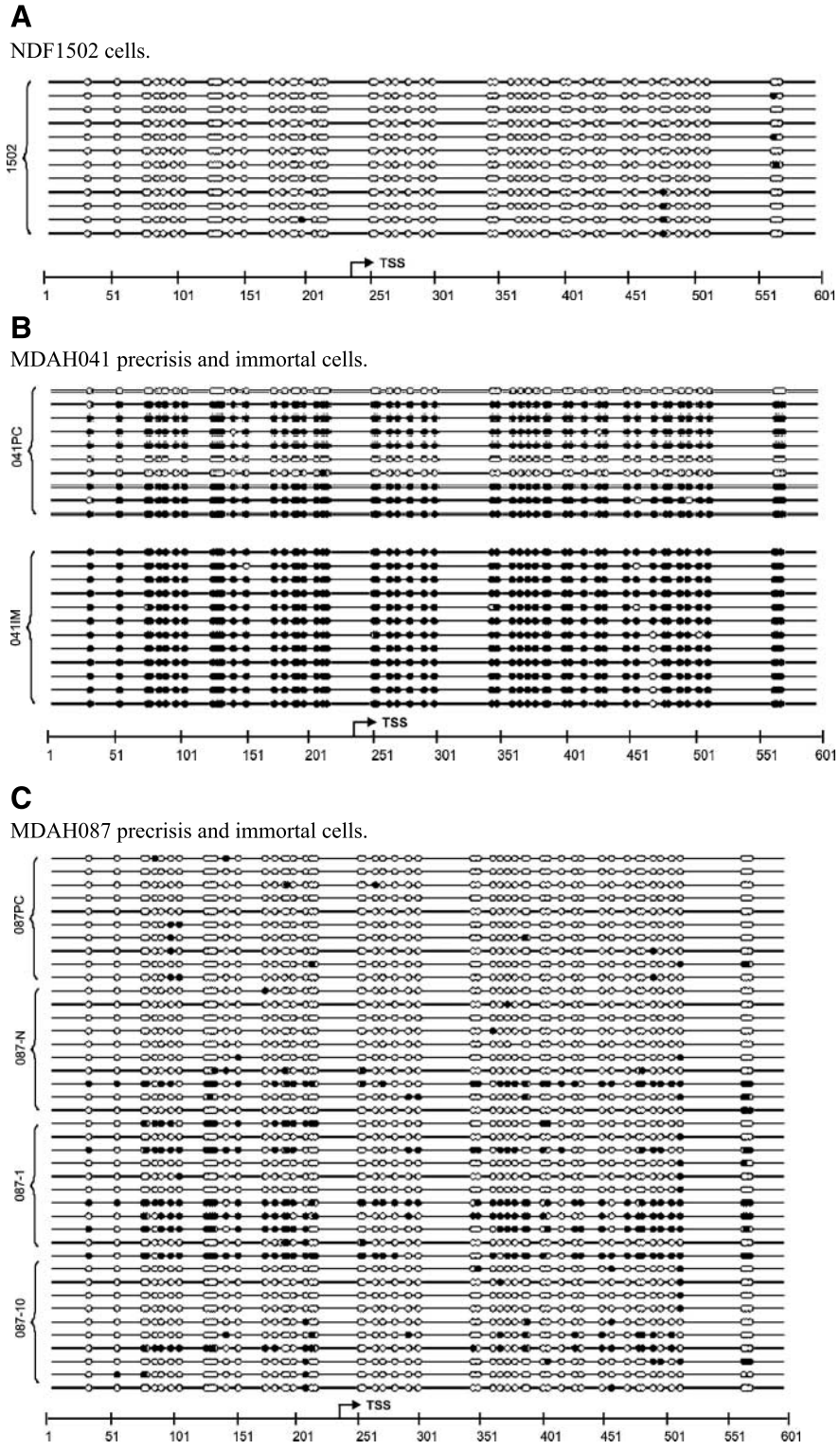

FIGURE 2. Bisulfite sequencing of the *IRF7* promoter. The methylation status of CpG islands in the *IRF7* promoter region in normal and LFS cells was examined by bisulfite sequencing. **A.** Bisulfite sequencing of the *IRF7* promoter in NDF1502 cells. **B.** Bisulfite sequencing of the *IRF7* promoter in precrisis and immortal MDAH041 cells. **C.** Bisulfite sequencing of the *IRF7* promoter in precrisis and immortal MDAH087 cells. Closed circles, methylated C in CpG dinucleotides; open circles, unmethylated C in CpG dinucleotides. TSS, transcription start site.

the control normal fibroblasts, NDF1502 (Fig. 2A and B). In MDAH087 cell lines, we found little methylation in the precrisis MDAH087 or MDAH087-N immortal cells, but there was hemimethylation in MDAH087-1 and MDAH087-10 immortal cells (Fig. 2C). Furthermore, we did observe loss of chromosome 11p (RP1-44H16-cM0.8 to AC134982.5-cM48.5), which corresponds to the location of *IRF7* sequences using comparative genomic hybridization (data not shown) in MDAH087-1 and MDAH087-10 cell lines. Because both mechanisms of IRF7 inactivation are observed, this indicates the importance

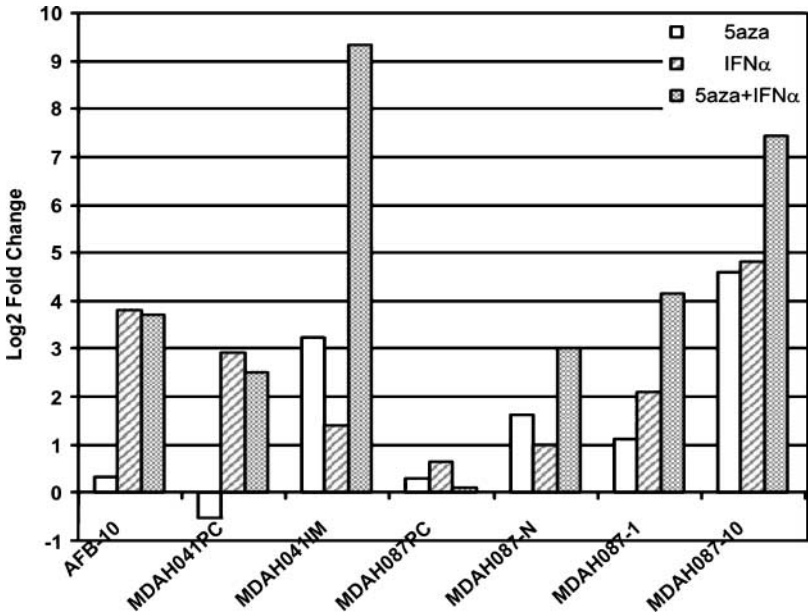

FIGURE 3. Demethylation potentiated the induction of *IRF7* gene expression by IFNα treatment on immortal MDAH041 fibroblast cells. Normal, precrisis, and immortal LFS cell lines were treated with 1 μmol/L 5-aza-dC or 1,000 units/mL IFNα for 2 d, in parallel with IFNα treatment with or without 5-aza-dC pretreatment. The individual and combined effects of 5-aza-dC and IFNα on IRF7 gene expression in normal and LFS cell lines were examined by quantitative RT-PCR. MDAH041PC, MDAH041 precrisis cells. MDAH041IM, MDAH041 immortal cells. *Y* axis, log 2 fold changes of *IRF7* gene expression after each treatment compared with untreated cells. MDAH087PC, MDAH087 precrisis cells. 5aza, 5-aza-dC treatment versus no treatment. IFNα, IFNα treatment versus no treatment. 5aza + IFNα, IFNα treatment with 5-aza-dC pretreatment versus no treatment.

of this genetic event, loss of IRF7, in immortalization. In addition, analysis of an EBV-immortalized lymphoblastoid cell line from patient MDAH041 and an immortal lymphoblastoid cell line from an affected sibling (MDAH275) indicated that the *IRF7* gene was also hemimethylated in these cell lines (data not shown). In contrast, genomic DNA prepared from fresh lymphoblasts of patient MDAH041 did not reveal any germ-line *IRF7* promoter methylation. However, no promoter methylation was detected for *IRF5* in any normal or LFS cell line (data not shown), suggesting a nonepigenetic mechanism in the down-regulation of IRF5 expression. Furthermore, although the expression of *TLR3, IFNβ*, and *OAS1* was also induced by 5-aza-dC treatment, no CpG island was revealed by MethPrimer software in their promoter regions (data not shown). This finding indicated that the induction of those ISGs might be an indirect result from the 5-aza-dC reactivation of the transcription factor *IRF7*, which was repressed through epigenetic silencing in our immortal LFS cells.

Effect of DNA Demethylation and IFNα Treatment on IRF7 Expression and Cell Proliferation

The epigenetically silenced IFN-regulated (or responsive) genes can be reactivated by 5-aza-dC, which is maximal following 6 days of 5-aza-dC treatment. To further evaluate DNA demethylation in the regulation of the IFN pathway, we examined the combined effects of 5-aza-dC and IFNα on *IRF7* gene expression in the four immortal LFS cell lines using a suboptimal 2-day treatment with 1 μmol/L 5-aza-dC alone as well as a combination treatment with 1,000 units/mL IFNα.

Consistent with the findings from the 6-day treatments, DNA demethylation with 5-aza-dC treatment for 2 days mildly induced *IRF7* gene expression in the four immortal LFS cells. Under these conditions, the expression level of *IRF7* was not significantly altered in normal AFB-10 fibroblasts or precrisis MDAH041 and MDAH087 fibroblasts (Fig. 3). A 2-day IFNα treatment alone increased *IRF7* expression in normal AFB-10, precrisis MDAH041 cells, and immortal MDAH087-1 and MDAH-10 cells, with only minor changes in immortal MDAH041, precrisis MDAH087, and immortal MDAH087-N cells. When those normal and LFS fibroblast cells were pretreated for 2 days with 5-aza-dC and then treated with IFNα, additive induction of *IRF7* gene was observed in all four immortal cell lines, with the strongest response in immortal MDAH041 cells. Combined treatment did not result in significantly more *IRF7* expression in normal AFB-10, precrisis MDAH041, and precrisis MDAH087 cells compared with 5-aza-dC or IFNα treatment alone. This indicated that the IFN induction of *IRF7* expression, an important regulator of the IFN pathway, was very sensitive to methylation status of its promoter. The combination of 5-aza-dC and IFNα potentiated the effects on gene expressions of *TLR3, IFNα, IFNβ, STAT1*, and *OAS1* (data not shown). The same expression patterns of those ISGs on 5-aza-dC and IFNα treatment also suggested that the absence of endogenous IFN production in immortal LFS cell lines might be due to promoter methylation of their key transcription factor, *IRF7*. Thus, epigenetic silencing of *IRF7* may be a critical step (early event) in the immortalization process.

This result supported our hypothesis that the impairment of the IFN pathway resulted from promoter methylation of the ISGs and could be restored by demethylation. This was also consistent with senescence-associated β-gal staining assay of the LFS cells after 5-aza-dC treatment (Fig. 4; ref. 26). In precrisis LFS cells, similar numbers of cells appeared senescent with or without 5-aza-dC treatment, whereas senescence-associated β-gal activity significantly increased ~2- to 8-fold in all four immortal cell lines after 5-aza-dC treatment (Fig. 4).

Because 5-aza-dC treatment was able to induce senescence and potentiate IFNα induction of *IRF7* expression, we tested whether 5-aza-dC and IFNα treatment had a similar effect on cell growth of immortal LFS cells. We used suboptimal doses of 5-aza-dC in combination with increasing concentrations

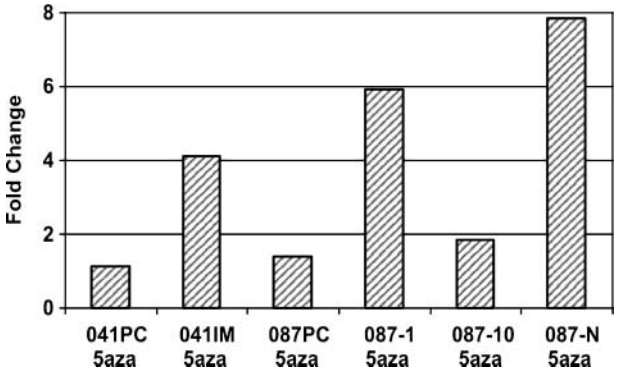

FIGURE 4. Increase of senescence of LFS fibroblast cells in senescence-associated β-gal assay after demethylation treatment. Senescence-associated β-gal assay was done on precrisis and immortal LFS cells after these cells were treated with 1 μmol/L 5-aza-dC for 6 d and then compared with untreated cells. Fold change, fold increase of blue staining for senescence-associated β-gal activity in 5-aza-dC–treated versus untreated cells.

(111, 333, and 1,000 units/mL) of IFNα. Compared with untreated immortal MDAH041 cells, treatment with either 5-aza-dC or IFNα suppressed cell growth in a dose-dependent manner (Fig. 5 and data not shown). This inhibition was potentiated by the combination of the two agents: IFNα combined with a low dose of 5-aza-dC treatment (0.1 μmol/L), which normally did not influence immortal MDAH041 cell growth, resulted in a greater reduction in cell number (~20% to ~45%) compared with IFNα treatment alone (~5% to ~30%; Fig. 5). Using poly(ADP-ribose) polymerase assay as a marker for cell death, we did not observe any cleavage of poly(ADP-ribose) polymerase in MDAH041 immortal LFS cells (data not shown), suggesting that no apoptosis occurred in this cell line on 5-aza-dC or IFNα treatment.

Disruption of Innate Immunity in Immortal LFS Fibroblasts

The IFN pathway is activated in normal cells by viral infection as part of the innate antiviral immune response, and cells that have a fully functional innate, antiviral system are able to protect themselves and neighboring cells against a low dose of virus, largely due to the induction of the protective IFN signaling cascade. Disruption of the IFN pathway often sensitizes cells to enhanced cytolytic responses following viral infections (50). Using a vesicular stomatitis virus sensitivity assay, we examined the state of the innate antiviral immune response in the immortal LFS cell lines. The immortal LFS cell lines generally displayed higher sensitivity to low-dose virus infection compared with control (AFB-10 cells) or precrisis LFS cells (Fig. 6A), suggesting that partial dysregulation of the antiviral signaling pathway had occurred during immortalization. However, all cell lines were sensitive to high-dose (multiplicity of infection, 5) virus infection, which probably overwhelmed their already dysfunctional IFN response pathway. The state of IFN dysregulation was also apparent following IFN pretreatment before virus infection. IFN pretreatment was able to protect all cells except the MDAH087-1 cell line (Fig. 6B), confirming that this cell line is unable to establish an IFN-inducible antiviral state and thus lacks a functional IFN signaling pathway. In summary, functional analysis by direct IFNα induction, polyI:C treatment, and vesicular stomatitis virus viral sensitivity assays all showed that the IFN pathway was disrupted after spontaneous immortalization of LFS cells.

Overexpression of IRF5 and IRF7 Can Reduce Proliferation and Induce Senescence in Immortal MDAH041 and MDAH087-1 LFS Fibroblast Cells

To address the role of IRF5 and IRF7 transcriptional activity in cellular mortality, we overexpressed IRF5 and IRF7 in immortal LFS fibroblasts. Immortal MDAH041 and MDAH087-1 cell lines were stably transfected with IRF5, IRF7, or both of these genes. After G418 selection for 14 days, the cells were harvested to measure the RNA and protein expression levels of IRF5 and IRF7, as well as other known IRF inducible genes (Table 3; Fig. 7). As expected, *IRF5* mRNA expression was up-regulated compared with the vector control (3.1-fold) in IRF5-transfected cells and *IRF7* mRNA was highly overexpressed (657-fold) in IRF7-transfected cells. Both IRF5 and

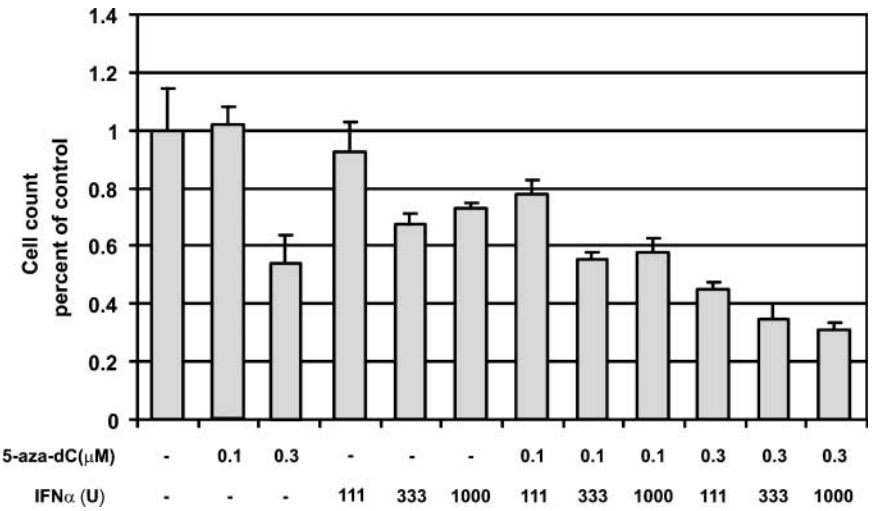

FIGURE 5. Demethylation potentiated the growth arrest effects of IFNα treatment on immortal MDAH041 fibroblast cells. Immortal MDAH041 cells were treated with different lower concentrations of 5-aza-dC (0.1 and 0.3 μmol/L), IFNα (111, 333, and 1,000 units/mL), or the combination of the two for 24 h. Cell growth rate was measured on the 6th day by counting cell numbers. Increasing concentration of IFNα inhibited cell growth to ~70% of untreated immortal MDAH041 cells; with 5-aza-dC pretreatment, IFNα treatment further reduced cell proliferation to ~50% of control.

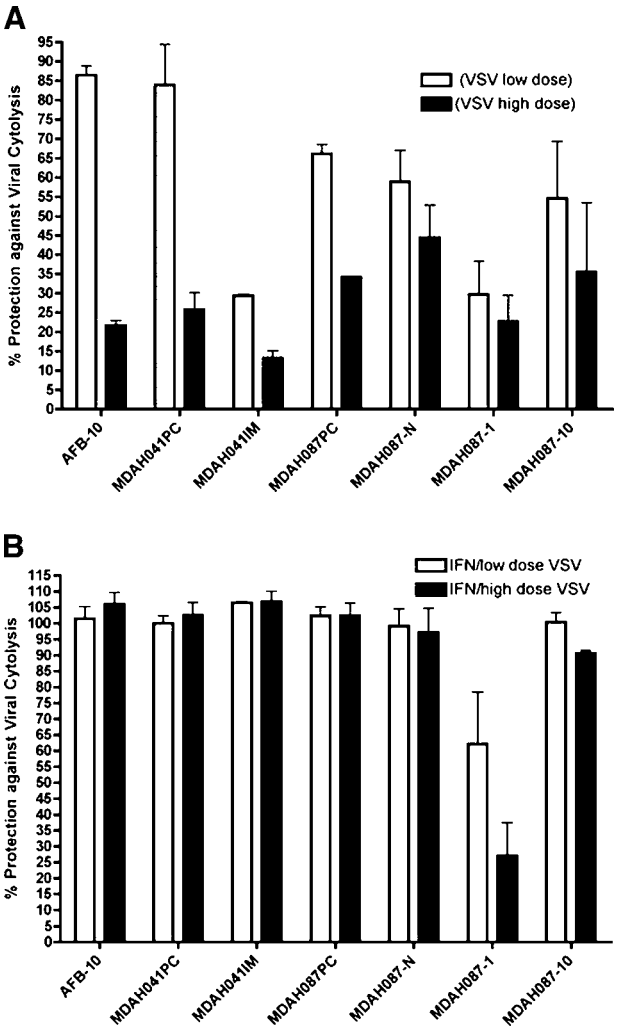

FIGURE 6. Virus sensitivity of normal and LFS fibroblast cells. Normal, precrisis, and immortal LFS cells were evaluated for their ability to induce an IFNα/β–induced antiviral response to vesicular stomatitis virus (*VSV*) infection by virus-induced cytopathicity using 3-(4,5-dimethylthiazol-2-yl)-2,5-diphenyltetrazolium bromide assay. The values were normalized to the value of control uninfected cells, which was set to 100% from at least two independent experiments (n = 8) with SD at <10%. **A.** Virus sensitivity assay of normal and LFS cell lines without IFNα pretreatment. **B.** Virus sensitivity assay of all the cell lines with IFNα pretreatment. MDAH041PC, MDAH041 precrisis cells; MDAH041IM, MDAH041 immortal cells; MDAH087PC, MDAH087 precrisis cells.

IRF7 were up-regulated albeit to a lesser extent in combined transfections of the two transcription factor partners (2.19-fold for *IRF5* and 572-fold for *IRF7*). Higher levels of expression of several ISGs were observed after transfection of IRF5 or IRF7 even without viral infection or polyI:C treatment. Expression of *IFNα, IFNβ, IRF7*, and *OAS1* was moderately elevated in IRF5 singly transfected cells. Slight increases in *IFNα* and *IFNβ* gene expression were observed in IRF7-overexpressing cells, whereas only *OAS1* was up-regulated in IRF5/IRF7–cotransfected cells (Table 3A). Western blot analysis confirmed the higher protein expression of IRF5 and/or IRF7 in the respective transfected cells (Fig. 7A and B). In contrast, no significant change in *TLR3* and *STAT1* mRNA or STAT1 protein expression was observed in any transfected cells, indicating that TLR3 and STAT1 are upstream of IRFs in the IFN signaling pathway.

To determine whether the kinetics of ISG expression was altered in IRF5- and IRF7-transfected cells on polyI:C stimulation, which mimics viral infection, RNA was harvested as a function of time after polyI:C treatment. A small increase in *IRF5* at 8 hours and in *IRF7* between 4 and 6 hours was seen in vector control cells. In IRF5 singly transfected cells, which already had higher expression levels of both *IRF5* and *IRF7*, additional induction of both genes was transiently observed when the cells were treated with polyI:C for only 1 hour. In IRF7 single transfectants that highly overexpressed the *IRF7* gene, we detected up-regulation of *IRF7* mRNA after 1 hour of polyI:C stimulation, which persisted until 6 hours. In IRF5/IRF7 double transfectants, additional increases of *IRF5*, but not *IRF7*, mRNA expression were observed at 2 and 6 h post-treatment (Table 3B). PolyI:C treatment for 8 hours activated *TLR3* in vector control cells, whereas as little as 1 hour of stimulation was sufficient to induce *TLR3* mRNA in IRF5-transfected and IRF5/IRF7–cotransfected cells. Similar gene expression patterns were detected for *IFNα* and *OAS1* mRNA. *IFNα* mRNA expression was only slightly up-regulated after 4 hours of polyI:C treatment and the mRNA returned to untreated levels at 24 hours in vector control cells. In IRF5-transfected cells, IFNα was briefly elevated after 1 hour of polyI:C treatment. In contrast, polyI:C treatment of IRF5/IRF7 double transfectants resulted in a similar but stronger induction of IFNα mRNA after 1 hour, and importantly, this induction persisted for 24 hours. *OAS1* mRNA was induced after 6 hours of polyI:C treatment in vector control cells, whereas its rapid (as early as 1 hour) and persistent up-regulation was observed after stimulation of either single or double transfectants (Table 3B). No significant differences were detected in the induction patterns of *STAT1* and *IFNβ* mRNA in any of the transfectants or vector control cells (data not shown). Overall, overexpression of IRF5 and IRF7 induced a rapid, stronger, and more persistent activation of the IFN pathway following polyI:C treatment.

As transcriptional mediators of virus- and IFN-induced signaling pathways, nuclear translocation is critical for the activation and function of IRF3 and IRF7 after viral infection or polyI:C treatment, whereas nuclear trafficking of IRF5 can only be induced by overexpression of TBK1 or IKKε (51, 52). No change of IRF3 expression was found in any of the four immortal MDAH cell lines excluding its involvement in the immortalization process. The expression pattern of IRF5 was found to be restricted to the cytoplasm in both control and IRF5-transfected cells even on polyI:C induction, which was similar to other researcher's findings (data not shown, refs. 51, 52). To determine the subcellular localization of IRF7 protein, immunostaining was done on immortal MDAH041 control and IRF7-transfected cells with or without polyI:C treatment. As expected, stronger immunofluorescence of IRF7 proteins was detected in IRF7-transfected cells, corresponding to its overexpression (Fig. 8). Without any activation, IRF7 immunofluorescence was located in both the nucleus and cytoplasm of IRF7-transfected cells (Fig. 8B, *first row*), whereas weak staining of IRF7 was found in the control cells and this was restricted to the cytoplasm (Fig. 8A, *first row*).

After 4 hours of polyI:C treatment, some positive IRF7 staining was observed in the nucleus of the untransfected control cells (Fig. 8A, *second row*), whereas in IRF7-transfected cells strong nuclear accumulation of IRF7 was detected, which colocalized with 4′,6-diamidino-2-phenylindole nucleus staining (Fig. 8B, *second row*). By 24 hours of polyI:C induction, IRF7 remained predominantly in the nucleus of both cells (Fig. 8A and B, *third row*). The significant localization of IRF7 protein in the nucleus of the transfected cells under basal conditions and its rapid nuclear translocation in response to polyI:C induction indicate that the overexpressed IRF7 protein was biologically activated without or with polyI:C treatment of the transfected cells.

To investigate whether IRF5 and IRF7 function as growth-suppressive genes, cell proliferation assays were carried out on single and double transfectants immediately following a 14-day drug selection. The overexpression of either IRF5 or IRF7 in immortal MDAH041 cells resulted in reduced proliferation rates compared with vector control cells (Fig. 9A). IRF5 and IRF7 transfectants also displayed reduced cell growth, ~85% and ~75% of that of vector control cells, respectively, whereas the combination of IRF5 and IRF7 showed the most growth inhibition, slowing the cell growth rate to ~65% compared with vector control cells. The IRF5-, IRF7-, and IRF5 + IRF7–transfected cells and vector control–transfected MDAH041 cells were cultured for over additional PD 30 (PD 0 started at day 14 after transfection) to examine the effect of these transcription factors on cellular life span. The continuous expression of IRF5 and/or IRF7 in the transfected cells was verified by Western blotting (data not shown). Consistent with cell proliferation assay shortly after transfection, the IRF5 and IRF7 MDAH041 single transfectants maintained a slower population doubling rate, which was further reduced in the double transfectant cells (Fig. 9C). Therefore, the overexpression of IRF5 and/or IRF7 reduced the growth rate of immortal MDAH041 cells. Interestingly, the level of expression of these transcription factors diminished during extended passage in culture (data not shown), consistent with their growth-suppressive activity (see Fig. 9A and B). Similar findings were observed in a parallel transfection study of MDAH087-1 cells (Fig. 9B and D).

Table 3. Quantitative RT-PCR Analysis of IRF5, IRF7, and IRF5 + IRF7 Overexpression in MDAH041 Cells

(A) IRF5, IRF7, and IRF5 + IRF7 Transfected vs Vector Control

	041IM pCMV-IRF5	041IM pCMV-IRF7	041IM pCMV-IRF5 + IRF7
TLR3	1.22	−1.88	−1.84
IFNα	4.35	2.00	−1.46
IFNβ	4.99	2.41	−1.13
IRF5	3.10	1.31	2.19
IRF7	6.23	657.11	572.05
STAT1	−2.14	−1.55	1.39
OAS1	5.94	1.04	4.44

(B) Time Course of PolyI:C Treated vs Untreated

	1 h	2 h	4 h	6 h	8 h	24 h
IRF5						
041IM pcDNA3.1	1.29	−1.55	1.82	1.59	2.99	1.83
041IM pCMV-IRF5	3.58	−1.02	1.24	1.48	−1.69	−3.10
041IM pCMV-IRF7	−1.29	−1.04	−1.75	−2.04	−1.20	−1.06
041IM pCMV-IRF5 + IRF7	1.25	4.17	−1.35	3.81	−1.37	−1.42
IRF7						
041IM pcDNA3.1	−4.69	1.01	2.20	5.10	1.85	1.88
041IM pCMV-IRF5	2.50	−1.02	1.12	−5.24	−2.19	−2.69
041IM pCMV-IRF7	2.03	2.46	1.84	2.10	−1.18	1.14
041IM pCMV-IRF5 + IRF7	1.41	1.46	1.69	1.07	−1.12	−1.21
TLR3						
041IM pcDNA3.1	−6.73	−4.50	1.04	1.47	3.34	39.40
041IM pCMV-IRF5	3.39	−1.40	1.64	1.71	1.49	17.39
041IM pCMV-IRF7	−1.26	1.28	−2.64	−1.61	0.67	6.63
041IM pCMV-IRF5 + IRF7	2.01	2.97	1.44	5.35	10.27	78.79
IFNα						
041IM pcDNA3.1	−3.34	−1.85	2.46	2.07	2.46	1.52
041IM pCMV-IRF5	3.25	−3.14	1.34	1.32	−1.34	−2.99
041IM pCMV-IRF7	−1.42	1.01	−2.51	−1.77	−1.10	1.20
041IM pCMV-IRF5 + IRF7	6.02	8.82	1.39	10.56	5.82	1.91
OAS1						
041IM pcDNA3.1	−2.75	1.68	−5.35	34.30	187.40	2,019.80
041IM pCMV-IRF5	2.00	4.00	5.06	19.29	29.24	685.02
041IM pCMV-IRF7	2.04	2.39	6.87	8.17	66.72	661.68
041IM pCMV-IRF5 + IRF7	1.14	2.14	12.21	32.90	95.67	694.58

NOTE: The immortal MDAH041 cells were transfected with pCMV-IRF5 and/or pCMV-IRF7 and treated with 100 μg/mL polyI:C for different periods of time (0, 1, 2, 4, 6, 8, and 24 h). Expression levels of *IRF5, IRF7*, and IRF-inducible genes were examined by quantitative RT-PCR. 041IM, MDAH041 immortal cells. (A) Transcription levels of *IRF5, IRF7*, and IRF-inducible genes in IRF5-, IRF7-, and IRF5 + IRF7–transfected immortal MDAH041 cells relative to pcDNA3.1 vector control immortal MDAH041 cells. (B) Time course of transcription levels of *IRF5, IRF7*, and IRF-inducible genes in stably transfected cells after polyI:C treatment compared with untreated cells.

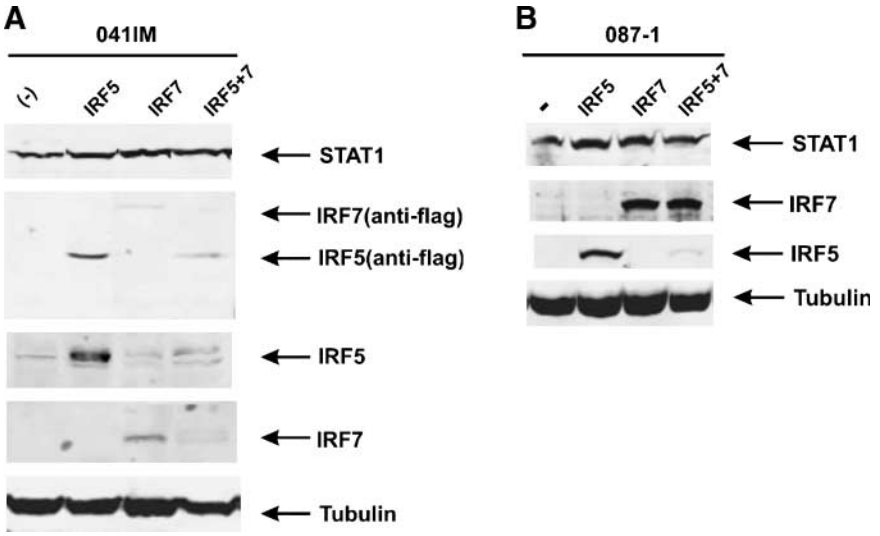

FIGURE 7. Western blot analysis of IRF5 and/or IRF7 overexpression in immortal MDAH041 and MDAH087-1 cells. The immortal MDAH041 and MDAH087-1 cells were stably transfected with pCMV-IRF5 and/or pCMV-IRF7. Protein expression levels of IRF5, IRF7, and STAT1 were analyzed by Western blots. Anti-flag antibody was applied to detect transfected IRF5 and IRF7 protein levels, whereas IRF5- and IRF7-specific antibodies were used for total IRF protein expression. **A.** Western blot analysis of IRF5 and/or IRF7 overexpression in immortal MDAH041 cells. **B.** Western blot analysis of IRF5 and/or IRF7 overexpression in MDAH087-1 cells. 041IM, immortal MDAH041 cells.

We also examined whether the overexpression of IRF5 and/or IRF7 could promote senescence in transfected immortal MDAH041 cells using the senescence-associated β-gal activity assay for detecting senescent cells. In cultures of precrisis MDAH041 cells (PD ~23) in which the majority of the cells are going into senescence, we observed that 43% of the cells displayed senescence-associated β-gal staining (Fig. 10A). The background staining in the cultures of MDAH041 immortal cells was ~5%. Stable transfection of each of the individual transcription factors, IRF5 or IRF7, induced an additional 5% senescence-associated β-gal staining over background. The combination of IRF5 with IRF7 was able to induce senescence-associated β-gal activity in 19.3% of the cells, which is equivalent to that observed in 5-aza-dC–treated immortal MDAH041 cultures. Similar results were observed in IRF5 + IRF7–overexpressing MDAH087-1 (Fig. 10B) cells.

Discussion

Immortalization is one of the earliest and essential cellular mechanisms associated with the onset of carcinogenesis. Microarray-based transcriptional profiling of the four immortal

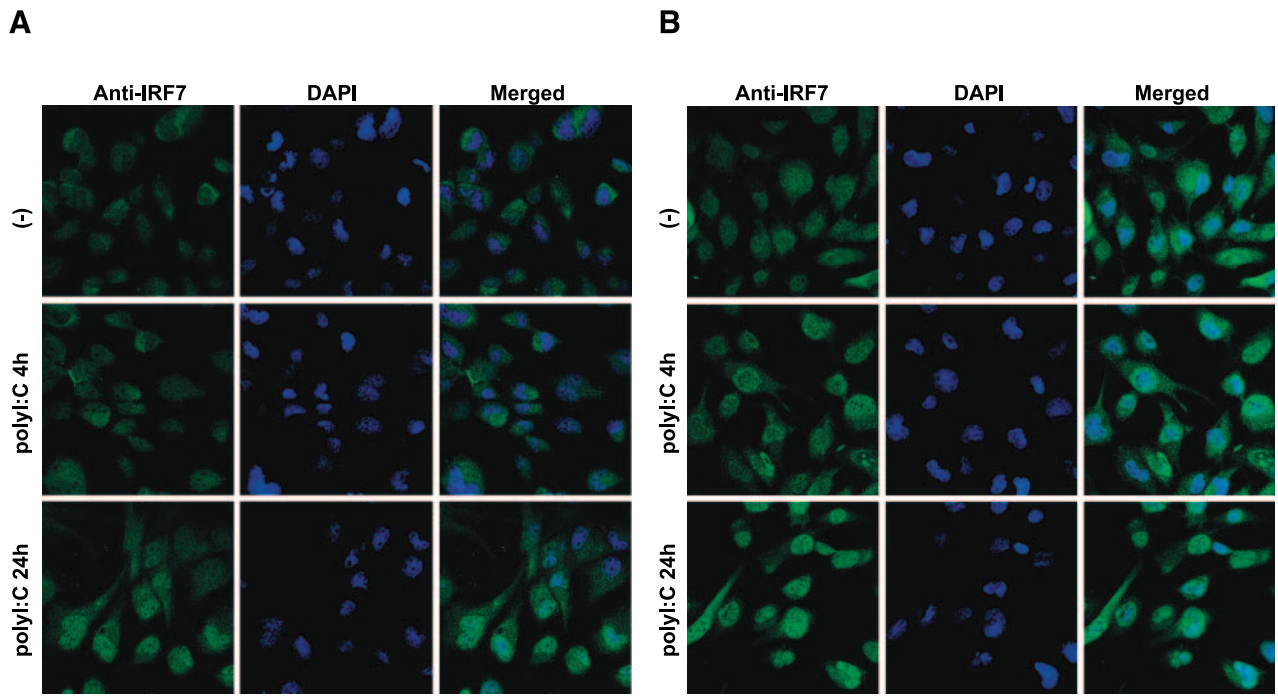

FIGURE 8. Nuclear translocation of IRF7 protein in immortal MDAH041 cells induced by polyI:C treatment. Subcellular localization of IRF7 was determined 4 and 24 h after polyI:C treatment by immunostaining. Nuclear translocation of IRF7 (*green*) induced by polyI:C treatment was evaluated by its colocalization with 4′,6-diamidino-2-phenylindole (*DAPI*) nuclear staining (*blue*). **A.** PolyI:C treatment of immortal MDAH041 control cells. **B.** PolyI:C treatment of immortal MDAH041 cells transfected with IRF7.

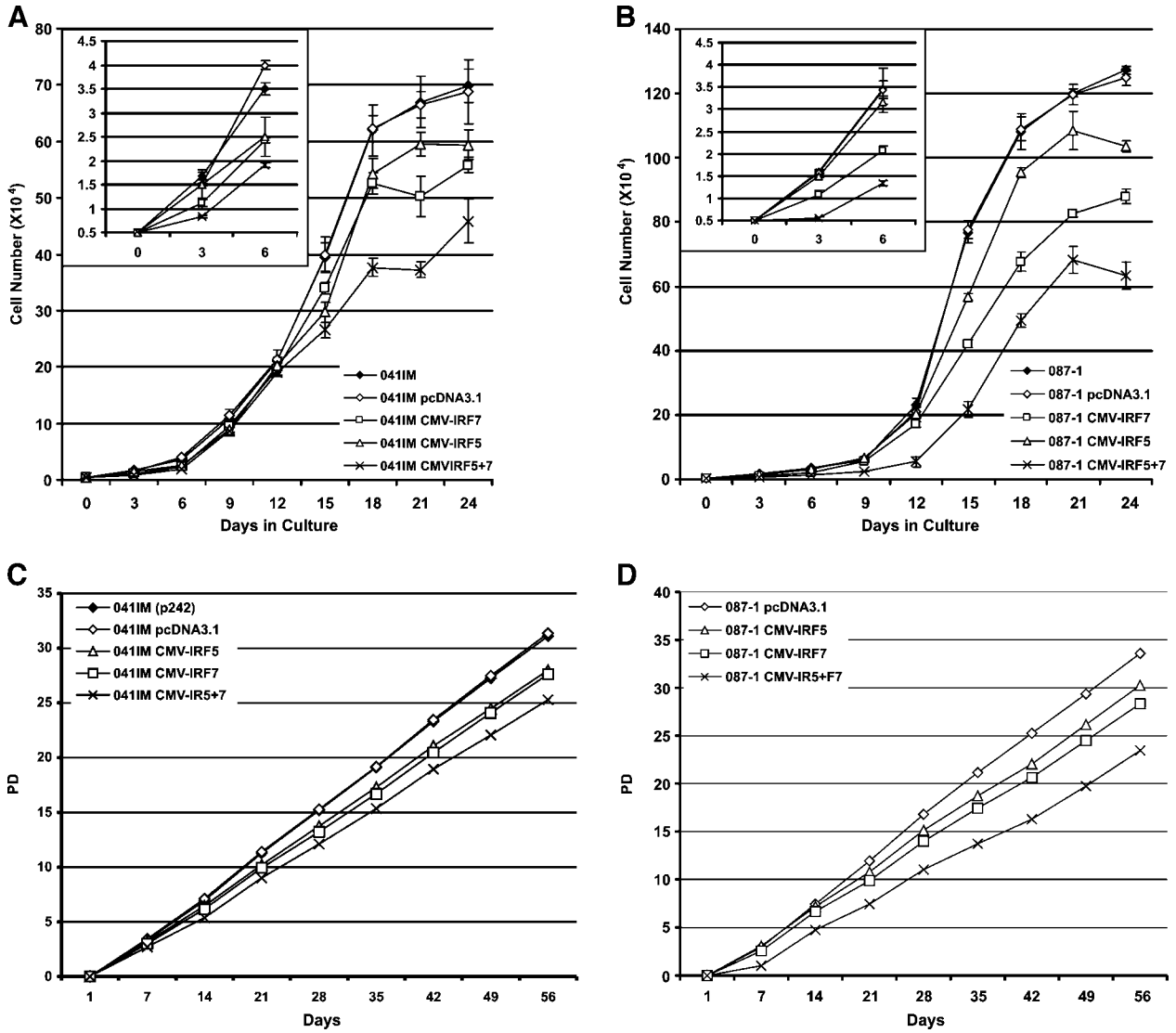

FIGURE 9. Overexpression of IRF7 induced growth arrest in immortal MDAH041 and MDAH087-1 fibroblast cells. **A** and **B.** Cell proliferation assays were done on IRF5-, IRF7-, and IRF5 + IRF7–transfected immortal MDAH041 cells (**A**) and MDAH087-1 cells (**B**) by counting cell numbers for both pcDNA3.1 vector control and IRF-transfected cells every 3 d for 24 d. Cell proliferation for the first 6 d were maximized and shown on the top left corner. **C** and **D.** IRF5-, IRF7-, and IRF5 + IRF7–transfected cells and vector control MDAH041 cells were cultured for over PD 30 (PD 0 started at day 14 after infection) to examine their cellular life span.

LFS cell lines revealed down-regulation of numerous IFN-regulated genes due to epigenetic silencing (10, 43). Here, we extended these findings by functional analysis of this pathway following treatment with IFNα and polyI:C, as well as evaluation of these cell lines in viral sensitivity assays. All of the four immortal LFS cell lines displayed defects in the IFN signaling pathway compared with precrisis LFS or normal human fibroblasts. Although the specific mechanisms of inactivation of the IFN pathway may be different among cell lines, the repression of this pathway seems to be a consistent feature of the four immortal LFS cell lines studied. The involvement of certain IFN pathway genes as tumor suppressors in carcinogenesis was further supported by the fact that overexpression of the transcription factors IRF5 and IRF7 was able to reverse the immortal phenotype and induce senescence, which was independent of the expression of telomerase. However, only mild up-regulation of ISG expression was found in IRF7- and IRF5 + IRF7–overexpressing cells without further stimulation, which indicated that the effect of both IRFs on growth inhibition and senescence was not directly related to the activity of the Janus-activated kinase/STAT signaling/IFN pathway because IRF7 is the master regulator of IFN type I genes. Furthermore, the defect of innate immunity could not be restored in these IRF-overexpressing cells (data not shown), supporting the notion that modulators other than the type I IFN pathway were involved in innate immunity.

Interestingly, we found that expression of the *IRF7* gene is repressed by promoter hypermethylation. A mixture of methylated and unmethylated alleles of *IRF7* was found in precrisis MDAH041, and it was nearly completely methylated

in immortal MDAH041 cells. This suggested that one allele of *IRF7* was already methylated in precrisis stage and the other allele was unmethylated until or during immortalization. As the cells progressed out of crisis and reached the stage of unrestricted growth, the second allele of *IRF7* in MDAH041 also acquired promoter methylation, which further led to complete suppression of *IRF7* gene expression. We are not able to exclude the possibility that the methylation detected in the *IRF7* promoter region in the second allele may be the result of gene conversion or chromosome translocation because no polymorphic marker was found in the promoter region of *IRF7*. Little *IRF7* promoter methylation was detected in the precrisis MDAH087 cells or MDAH087-N immortal cells, whereas in MDAH087-1 and MDAH087-10 immortal cells, there was loss of chromosome 11p15, detected by comparative genomic hybridization (data not shown), in addition to promoter hemimethylation. Therefore, both chromosome loss and epigenetic mechanisms account for the repression of the *IRF7* gene in those two immortal cell lines (MDAH087-1 and MDAH087-10).

IRF7 is located at 11p15.5, a well-known region containing several imprinted genes including *H19* and *IGF2* (53). However, bisulfite sequencing of DNA from fresh lymphoblasts of MDAH041 indicated no germ-line *IRF7* promoter methylation, although hemimethylation was observed in the *IRF7* promoter regions of EBV-immortalized MDAH041 lymphoblasts and MDAH275 lymphoblasts (an affected sibling of patient MDAH041) as well as precrisis MDAH041 fibroblasts. This excluded the possibility of germ-line imprinting of *IRF7* gene in these high-risk cancer patients and suggested that promoter methylation might be one of the early steps in spontaneous cellular immortalization and in EBV-mediated immortalization as well. Interestingly, although both *IRF7* and IFN inducible 9-27 (*IFITM1*) are located within 300 kbp of this well-known imprinted region, only *IRF7* has significant CpG islands in its promoter region. *IRF7* expression was not inducible by IFNα or polyI:C treatment, whereas *IFITM1* expression was responsive to IFNα treatment (data not shown). *IRF5* is located at 7q32, another chromosomal region known to harbor several imprinted genes. However, similar to another transcription factor in the IFN pathway (*STAT1*; ref. 43), we found no significant CpG methylation in the *IRF5* promoter region although large CpG islands are present. We suspect that the reduced expression of *IRF5* and *STAT1* during immortalization was regulated through other genes directly regulated by methylation or by indirect mechanisms, possibly through an IRF7-mediated transcriptional control mechanism.

Double-stranded RNA treatment (polyI:C) and IFNα stimulation had similar but distinct effects on IRF7 and IRF5 gene expression. The differential impairment of ISG expression indicated that different ISG expression changes contributed to the disruption of the IFN pathway but the specific defects in

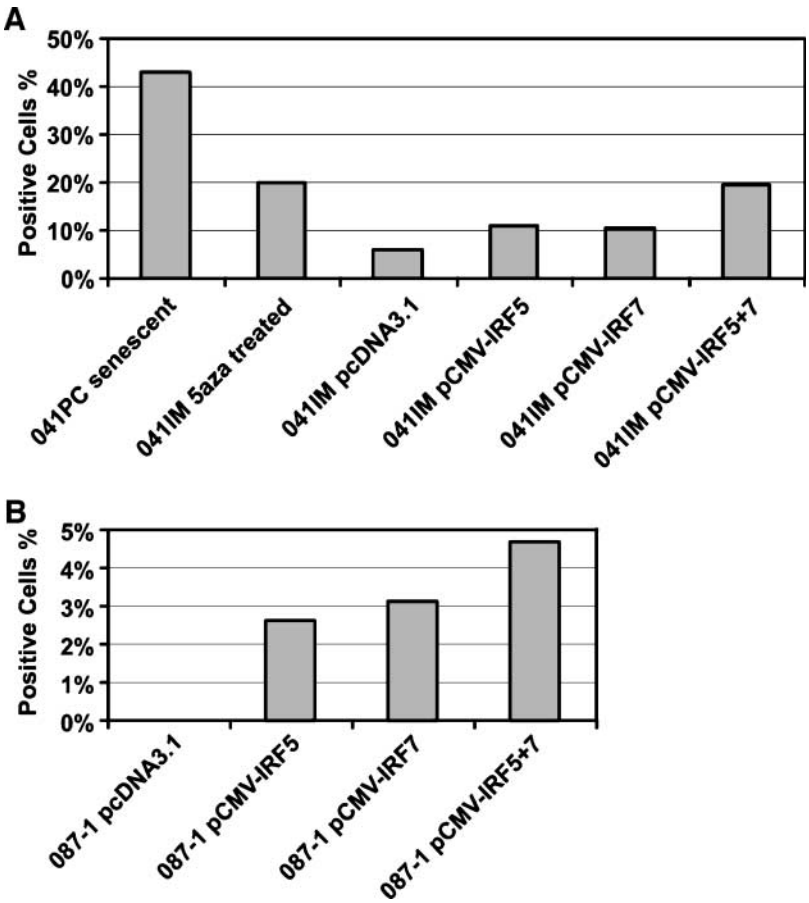

FIGURE 10. Overexpression of IRF5 and/or IRF7 induced senescence in immortal MDAH041 and MDAH087-1 fibroblast cells. Senescence-associated β-gal staining was done on pcDNA3.1 vector control, IRF5, IRF7, and IRF5 + IRF7 stably transfected cells. MDAH041 senescent cells and 5-aza-dC–treated immortal MDAH041 cells were used as positive controls. **A.** β-Gal assay of IRF5-, IRF7-, and IRF5 + IRF7–overexpressing immortal MDAH041 cells. **B.** β-Gal assay of IRF5-, IRF7-, and IRF5 + IRF7–overexpressing MDAH087-1 cells. Positive cells (%), percentage of cells that are positive for senescence-associated β-gal staining.

IFN signaling vary among the immortal LFS cell lines. Possibly, double-stranded RNA and IFNα trigger similar but nonidentical signaling pathways among the four immortal cell lines. This hypothesis was supported by a recent study in which it was shown that two distinct signaling pathways could modulate the transcriptional activity of IRF7. In cells with IFNα/β or Janus-activated kinase/STAT gene inactivation, *IRF7* genes can still be induced by complex formation of IRF3 with cyclic AMP–responsive element binding protein–binding protein and p300 independent of IFN signaling (54).

Overexpression of IRF5 and IRF7 resulted in elevation of several ISGs in the absence of polyI:C treatment, suggestive of double-stranded RNA–independent signaling events. Furthermore, in the IRF-transfected LFS immortal cells, a more rapid and more robust activation of the IFN pathway was observed on polyI:C stimulation, suggesting partial restoration of the abrogated IFN signaling pathway. As direct transducers of antiviral responses, IRF5 and IRF7 induce the expression of different subtypes of IFNα genes (37). Although they share similar signaling systems, the differential expression patterns and kinetics of ISGs on polyI:C induction in IRF5- or IRF7-transfected immortal LFS cell lines indicated that they might have nonredundant roles in both innate immune responses and cell cycle control. Consistent with our observations, a recent study comparing the differences of the gene expression profiles between IRF5- and IRF7-transfected BJAB cells found that distinct sets of genes were induced by IRF5 and IRF7 (55). In addition, there was a large number of overlapping genes induced by these factors. The stimulation of several cell cycle regulatory genes in both IRF5- and IRF7-overexpressing cells was consistent with the growth inhibition roles we found in our immortal LFS cells.

Another transcription factor, IRF3, which is a binding partner of IRF5 and IRF7, also plays a critical role in the regulation of IFN and IFN-inducible genes. However, neither the mRNA nor protein level of IRF3 was altered in any of the four LFS immortal cell lines (data not shown), which excluded its direct involvement during the immortalization process of LFS cells. In addition to IRF5 and IRF7, we have also examined the effect of ectopic expression of another key IFN regulatory factor, STAT1, on cellular mortality (43). Although not epigenetically regulated, STAT1 mRNA and protein expression were also down-regulated in immortal MDAH041 cells and up-regulated by DNA demethylation treatment (43). Overexpression of the transcription factors IRF5 and IRF7s did not increase STAT1 expression level in our experiments, which was consistent with the findings of others that STAT1 functions upstream of IRFs (29, 31). Unlike IRF5 and IRF7, reexpression of STAT1 alone was not able to affect growth rate, immortality, or induce senescence in immortal MDAH041 cells (43). Thus, immortalization may result from defects downstream of STAT1 in the signaling pathway, but this does not exclude the possibility that additional coactivators or binding partners such as STAT2/IRF9 are necessary.

The process of immortalization clearly involves several genetic events and impairment of multiple signal pathways. The precrisis LFS fibroblasts used in our study only have one copy of the wild-type tumor suppressor gene *p53*, which is lost on immortalization. However, loss of the wild-type *p53* gene is not sufficient for immortalization to occur, and additional events are required for cells to escape senescence and immortalize (8). Another tumor suppressor gene, $p16^{INK4a}$, the cyclin-dependent kinase inhibitor of retinoblastoma (RB) protein phosphorylation, has been reported to be epigenetically silenced in cancer and immortal cell lines and up-regulated in senescence human fibroblasts (56-58). In our LFS fibroblasts, loss of $p16^{INK4a}$ through both genetic and epigenetic mechanisms may also be an important contributing factor in immortalization, as two of the four cell lines (immortal MDAH041 and MDAH087-N cells) had inactivated $p16^{INK4a}$ as evidenced by promoter hypermethylation of one allele and gene deletion of the other allele, whereas the other two cell lines (MDAH087-1 and MDAH087-10 cells) had incurred biallelic gene deletion of $p16^{INK4a}$ (10). Furthermore, in addition to the significant role that the IFN pathway plays in immortalization, we identified two other pathways, cell cycle and cytoskeletal, which were also disrupted in the immortalization process (10).

In summary, this study showed a critical role for the transcription factors IRF5 and IRF7 in the suppression of the IFN pathway during cellular immortalization. Reactivation of IFN-regulated genes by overexpression of these transcription factors or demethylation of their promoters was sufficient to induce senescence. Therefore, cellular immortality and senescence are reversible traits that are controlled by multiple mechanisms including cell cycle control, cytoskeletal proteins, and the IFN pathway.

Materials and Methods

Cell Culture

The NDF1502 cells, MDAH041 cell lines, and MDAH087 cell lines used in this study and their culture conditions were previously described (26). The MDAH fibroblast cells, which came from two LFS patients and have limited life span, were named precrisis cells (PC) in contrast to the spontaneously immortalized cell lines (IM). Precrisis MDAH041 cells were cultured from PD 13 up to PD 23. Precrisis MDAH041 cells begin to accumulate senescent cells after PD 20 but remained viable with reduced proliferation and a characteristic large, flattened senescent morphology. These cells (PD 23) were defined as senescent cells and were used for quantitative RT-PCR and Western blots. Normal adult dermal fibroblasts (AFB-10) were established from fresh tissue samples,[4] and by PD 21 of culturing, exhibited numerous senescent cells. RNA from normal human fibroblasts HCA2 (PD 75) at the time of senescence was a kind gift from Dr. James R. Smith.

5-aza-dC, polyI:C, and IFNα Treatment

Treatment of all the cells with 5-aza-dC (Sigma-Aldrich, Inc.) for microarray and quantitative RT-PCR experiments followed the protocol described earlier (10, 26).

PolyI:C (Amersham Biosciences Corp.) was diluted according to the manufacturer's instruction, and 100 μg/mL polyI:C was applied on IRF-transfected cells for different time periods (1, 2, 4, 6, 8, and 24 h). The untreated control cells were changed with fresh medium for 24 h before total RNA was harvested.

[4] M.A. Tainsky, unpublished data.

Cells were treated with IFNα (Biosource International, Inc.) and/or 5-aza-dC: (*a*) 1 μmol/L 5-aza-dC in MEM for 2 d; (*b*) 1,000 units/mL IFNα in MEM for 2 d, with medium changed on day 3 to regular MEM for 2 more days; or (*c*) 1 μmol/L 5-aza-dC in MEM for 2 d, with medium changed on day 3 to MEM with 1,000 units/mL IFNα. On the 5th day, total RNA and proteins were isolated for quantitative RT-PCR and Western blots.

To examine whether 5-aza-dC synergistically promotes the effects of IFNα on cell growth, immortal MDAH041 cells were treated with lower concentrations of 5-aza-dC (0.1 and 0.3 μmol/L), IFNα (111, 333, and 1,000 units/mL), or the combinations of 5-aza-dC and IFNα for 24 h. Cell growth rate was measured on the 6th day by counting the cell numbers. Each treatment was done in triplicate wells and each experiment was repeated at least twice. Results represented the percentage of cell counts compared with untreated control cells at the indicated treatment.

Senescence-Associated β-Gal Staining Assay

The senescence-associated β-gal assay was done as previously described (43). Five independent fields were randomly chosen and analyzed for counting the stained cells. Each field included at least 50 cells.

Quantitative RT-PCR

Total RNA was extracted from each experiment with the Qiagen RNeasy Kit. Two micrograms total RNA were reverse transcribed into cDNA using Superscript II (Invitrogen). Quantitative RT-PCR was done with SYBR Green PCR Detection kit (PE Biosystems) as previously described (26). The relative fold change of the gene of interest is calculated by normalizing it to an endogenous gene, *GAPDH*, which was not changed during various treatments, and comparing it with its control sample [$2^{-\Delta\Delta C_t}$, where $\Delta\Delta C_t = (C_{t\ \text{gene of interest}} - C_{t\ GAPDH})_{\text{experiment}} - (C_{t\ \text{gene of interest}} - C_{t\ GAPDH})_{\text{control}}$]. The primer sets used are listed in Supplementary Table S1. For each experiment, two independent RNA preparations as biological replicates were used and revealed the same trend. Triplicate wells were done in each individual experiment and the results were expressed as the average of those three wells with <5% SD. Only one representative experiment was chosen to be presented in the article.

Western Blots

Western blots were done as described (10, 43) using 50 μg of cell extracts from normal and LFS cells. The primary antibodies used in our study were anti-IRF5 (Abcam, Inc.); anti-STAT1, anti-IRF7, and anti–α-tubulin (Santa Cruz Biotechnology, Inc.); anti–phospho-STAT1 (Tyr^{701}; Cell Signaling Technology, Inc.); and anti-flag M2 antibody (Sigma-Aldrich). The Alexa Fluor 680–labeled secondary antibodies were from Molecular Probes and the Li-Cor IRDye 800–labeled secondary antibodies were from Rockland Immunochemicals. The signal was then detected using the Odyssey Infrared Imaging System (Li-Cor Biosciences).

PCR Amplification, Cloning, and Sequencing of Bisulfite-Modified Genomic DNA

Genomic DNAs were prepared with the Puregen DNA isolation kit (Gentra System). Genomic DNA (1 μg) was denatured and treated with 3.6 mol/L sodium bisulfite as described (43). The sodium bisulfite–modified genomic DNA was suspended in 50 μL of water and 10 μL of DNA were amplified by PCR with two nested PCR reactions. The annealing temperature was 56°C for the first PCR and 58°C for the second PCR (IRF7). The two sets of primers were F1, 5′ GTAAGGGTTTTTGTCGTAGTAGACGTTAG (−510), and R1, 5′ AACGTAATAATTCATACCTATAATCCCAAC (+460); F2, 5′ GGTTATAGGTGTGATTGTAGGTGTG (+376), and R2, 5′ CCCTAAACTATAATAAAATAACTCCATCTC (−221).

The numbers in parentheses indicate the relevant position to the transcription start site of *IRF7* (NM001572). The PCR products were cloned into pCR2.1-TOPO vector (Invitrogen Life Technologies) using the TOPO-TA Cloning Kit (Invitrogen Life Technologies). Ten clones for each PCR were subjected to double-strand DNA sequencing using M13-reverse and T7 primer on the vector. To avoid clonal bias in the PCR products, the bisulfite treatment and subsequent PCR and sequencing were repeated at least once as an independent DNA preparation.

Transfection of IRF5 and/or IRF7 into Immortal MDAH041 and MDAH087-1 Cells

pCMV-IRF5 and pCMV-IRF7 vectors were kind gifts from Dr. Paula M. Pitha. pCMV-IRF5, pCMV-IRF7, or the combination of these two vectors was transfected into immortal MDAH041 and MDAH087-1 cells using Lipofectamine reagent (Invitrogen Life Technologies) according to the manufacturer's instructions. After 48 h of transfection, the cells were selected in growth medium with 200 μg/mL G418. The stably transfected cells were also treated with polyI:C as described earlier. Two independent transfection experiments were done and representative data from one of the experiments are shown in Results.

Subcellular Localization of IRF7 Proteins

Immortal MDAH041 control and IRF7-overexpressing cells were seeded on coverslips and treated with 100 μg/mL polyI:C for 4 or 24 h. Cells were then fixed with fresh 3.7% formaldehyde and then permeabilized in 0.25% Triton X-100/PBS, blocked in 5% donkey serum/PBS, and incubated with anti-IRF7 antibody (in donkey serum, 1:100 dilution) for 1 h, followed by 1-h incubation with Alexa Fluor 488 secondary antibody (1: 200 dilution; Invitrogen Life Technologies). Coverslips were then mounted in Prolong Gold antifade reagent with 4′,6-diamidino-2-phenylindole (Invitrogen Life Technologies) and examined under a fluorescence microscope. All pictures were taken at a magnification of ×40.

Proliferation and Life Span Assays

pCMV-IRF5– and/or pCMV-IRF7–transfected cells were seeded in 24-well plates (5×10^3 per well) at 14 d after transfection. A hemocytometer was used to count cell numbers every 3 d for the next 24 d. The experiment was done in triplicate wells and each experiment was repeated at least twice. The results were shown as the average cell number of the three wells with SD at <10%. Life span assay was also done by continuously culturing those transfected cells over PD 30 as described earlier (43).

Virus Sensitivity Assay

Cells were seeded in 96-well plates at a density of 1×10^4 to 2×10^4 per well and cultured overnight in the presence or absence of IFNα (1,000 units/mL). The cells were then infected with a low dose (multiplicity of infection, 0.05) or high dose (multiplicity of infection, 5.0) of vesicular stomatitis virus (Indiana strain) for 1 h. Virus-induced cytopathicity was determined by a 3-(4,5-dimethylthiazol-2-yl)-2,5-diphenyltetrazolium bromide assay as previously described (43). Results were expressed as relative values of cell viability compared with control uninfected cells (set as 100) using Prism software (GraphPad, Inc.).

Acknowledgments

We thank Dr. James R. Smith (The University of Texas Health Science Center, San Antonio, TX) for his kind gift of senescent normal human HCA2 fibroblasts; Dr. Louise C. Strong (The University of Texas, M. D. Anderson Cancer Center, Houston, TX) for the kind gift of DNA from blood lymphocytes from patient MDAH041; Dr. Paula M. Pitha (Johns Hopkins University, Baltimore, MD) for her kind gift of the IRF5 and IRF7 vectors; and Alexei Ionan for his technical support on data analysis.

References

1. Hayflick L. The limited *in vitro* lifetime of human diploid cell strains. Exp Cell Res 1965;37:614–36.

2. Dimri GP, Lee X, Basile G, et al. A biomarker that identifies senescent human cells in culture and in aging skin *in vivo*. Proc Natl Acad Sci U S A 1995;92:9363–7.

3. Roninson IB. Tumor cell senescence in cancer treatment. Cancer Res 2003;63:2705–15.

4. Li FP, Fraumeni JF, Jr. Rhabdomyosarcoma in children: epidemiologic study and identification of a familial cancer syndrome. J Natl Cancer Inst 1969;43:1365–73.

5. Varley JM. Germline TP53 mutations and Li-Fraumeni syndrome. Hum Mutat 2003;21:313–20.

6. Malkin D, Li FP, Strong LC, et al. Germ line p53 mutations in a familial syndrome of breast cancer, sarcomas, and other neoplasms. Science 1990;250:1233–8.

7. Bischoff FZ, Strong LC, Yim SO, et al. Tumorigenic transformation of spontaneously immortalized fibroblasts from patients with a familial cancer syndrome. Oncogene 1991;6:183–6.

8. Bischoff FZ, Yim SO, Pathak S, et al. Spontaneous abnormalities in normal fibroblasts from patients with Li-Fraumeni cancer syndrome: aneuploidy and immortalization. Cancer Res 1990;50:7979–84.

9. Neumeister P, Albanese C, Balent B, et al. Senescence and epigenetic dysregulation in cancer. Int J Biochem Cell Biol 2002;34:1475–90.

10. Fridman AL, Tang L, Kulaeva OI, et al. Expression profiling identifies three pathways altered in cellular immortalization: interferon, cell cycle, and cytoskeleton. J Gerontol A Biol Sci Med Sci 2006;61:879–89.

11. Gollahon LS, Kraus E, Wu TA, et al. Telomerase activity during spontaneous immortalization of Li-Fraumeni syndrome skin fibroblasts. Oncogene 1998;17:709–17.

12. Shemer R, Birger Y, Dean WL, et al. Dynamic methylation adjustment and counting as part of imprinting mechanisms. Proc Natl Acad Sci U S A 1996;93:6371–6.

13. Robertson KD. DNA methylation and chromatin—unraveling the tangled web. Oncogene 2002;21:5361–79.

14. Kremenskoy M, Kremenska Y, Ohgane J, et al. Genome-wide analysis of DNA methylation status of CpG islands in embryoid bodies, teratomas, and fetuses. Biochem Biophys Res Commun 2003;311:884–90.

15. Deobagkar DD, Chandra HS. The inactive X chromosome in the human female is enriched in 5-methylcytosine to an unusual degree and appears to contain more of this modified nucleotide than the remainder of the genome. J Genet 2003;82:13–6.

16. Wilson VL, Jones PA. DNA methylation decreases in aging but not in immortal cells. Science 1983;220:1055–7.

17. House MG, Wistuba II, Argani P, et al. Progression of gene hypermethylation in gallstone disease leading to gallbladder cancer. Ann Surg Oncol 2003;10:882–9.

18. Yanagawa N, Tamura G, Oizumi H, et al. Promoter hypermethylation of tumor suppressor and tumor-related genes in non-small cell lung cancers. Cancer Sci 2003;94:589–92.

19. Baylin SB, Herman JG, Graff JR, et al. Alterations in DNA methylation: a fundamental aspect of neoplasia. Adv Cancer Res 1998;72:141–96.

20. Baylin SB, Herman JG. DNA hypermethylation in tumorigenesis: epigenetics joins genetics. Trends Genet 2000;16:168–74.

21. Esteller M, Corn PG, Baylin SB, Herman JG. A gene hypermethylation profile of human cancer. Cancer Res 2001;61:3225–9.

22. Paz MF, Fraga MF, Avila S, et al. A systematic profile of DNA methylation in human cancer cell lines. Cancer Res 2003;63:1114–21.

23. Sato N, Fukushima N, Maitra A, et al. Discovery of novel targets for aberrant methylation in pancreatic carcinoma using high-throughput microarrays. Cancer Res 2003;63:3735–42.

24. Vogt M, Haggblom C, Yeargin J, et al. Independent induction of senescence by p16INK4a and p21CIP1 in spontaneously immortalized human fibroblasts. Cell Growth Differ 1998;9:139–46.

25. Haaf T. The effects of 5-azacytidine and 5-azadeoxycytidine on chromosome structure and function: implications for methylation-associated cellular processes. Pharmacol Ther 1995;65:19–46.

26. Kulaeva OI, Draghici S, Tang L, et al. Epigenetic silencing of multiple interferon pathway genes after cellular immortalization. Oncogene 2003;22:4118–27.

27. Platanias LC. Interferons: laboratory to clinic investigations. Curr Opin Oncol 1995;7:560–5.

28. Stark GR, Kerr IM, Williams BR, et al. How cells respond to interferons. Annu Rev Biochem 1998;67:227–64.

29. Mamane Y, Heylbroeck C, Genin P, et al. Interferon regulatory factors: the next generation. Gene 1999;237:1–14.

30. Nguyen H, Hiscott J, Pitha PM. The growing family of interferon regulatory factors. Cytokine Growth Factor Rev 1997;8:293–312.

31. Doyle S, Vaidya S, O'Connell R, et al. IRF3 mediates a TLR3/TLR4-specific antiviral gene program. Immunity 2002;17:251–63.

32. Marie I, Durbin JE, Levy DE. Differential viral induction of distinct interferon-α genes by positive feedback through interferon regulatory factor-7. EMBO J 1998;17:6660–9.

33. Au WC, Moore PA, LaFleur DW, et al. Characterization of the interferon regulatory factor-7 and its potential role in the transcription activation of interferon A genes. J Biol Chem 1998;273:29210–7.

34. Sato M, Hata N, Asagiri M, et al. Positive feedback regulation of type I IFN genes by the IFN-inducible transcription factor IRF-7. FEBS Lett 1998;441:106–10.

35. Lu R, Au WC, Yeow WS, et al. Regulation of the promoter activity of interferon regulatory factor-7 gene. Activation by interferon snd silencing by hypermethylation. J Biol Chem 2000;275:31805–12.

36. Fukasawa M, Kimura M, Morita S, et al. Microarray analysis of promoter methylation in lung cancers. J Hum Genet 2006;51:368–74.

37. Barnes BJ, Moore PA, Pitha PM. Virus-specific activation of a novel interferon regulatory factor, IRF-5, results in the induction of distinct interferon α genes. J Biol Chem 2001;276:23382–90.

38. Barnes BJ, Kellum MJ, Pinder KE, et al. Interferon regulatory factor 5, a novel mediator of cell cycle arrest and cell death. Cancer Res 2003;63:6424–31.

39. Heylbroeck C, Balachandran S, Servant MJ, et al. The IRF-3 transcription factor mediates Sendai virus-induced apoptosis. J Virol 2000;74:3781–92.

40. Mori T, Anazawa Y, Iiizumi M, et al. Identification of the interferon regulatory factor 5 gene (IRF-5) as a direct target for p53. Oncogene 2002;21:2914–8.

41. Tamura T, Ishihara M, Lamphier MS, et al. An IRF-1-dependent pathway of DNA damage-induced apoptosis in mitogen-activated T lymphocytes. Nature 1995;376:596–9.

42. Tanaka N, Taniguchi T. The interferon regulatory factors and oncogenesis. Semin Cancer Biol 2000;10:73–81.

43. Tang L, Roberts PC, Kraniak JM, et al. Stat1 expression is not sufficient to regulate the interferon signaling pathway in cellular immortalization. J Interferon Cytokine Res 2006;26:14–26.

44. Yaar M, Karassik RL, Schnipper LE, Gilchrest BA. Effects of α and β interferons on cultured human keratinocytes. J Invest Dermatol 1985;85:70–4.

45. Damdinsuren B, Nagano H, Wada H, et al. Stronger growth-inhibitory effect of interferon (IFN)-β compared with IFN-α is mediated by IFN signaling pathway in hepatocellular carcinoma cells. Int J Oncol 2007;30:201–8.

46. Bielenberg DR, McCarty MF, Bucana CD, et al. Expression of interferon-β is associated with growth arrest of murine and human epidermal cells. J Invest Dermatol 1999;112:802–9.

47. Dong Z, Greene G, Pettaway C, et al. Suppression of angiogenesis, tumorigenicity, and metastasis by human prostate cancer cells engineered to produce interferon-β. Cancer Res 1999;59:872–9.

48. Sidky YA, Borden EC. Inhibition of angiogenesis by interferons: effects on tumor- and lymphocyte-induced vascular responses. Cancer Res 1987;47:5155–61.

49. Li LC, Dahiya R. MethPrimer: designing primers for methylation PCRs. Bioinformatics 2002;18:1427–31.

50. Balachandran S, Roberts PC, Kipperman T, et al. α/β interferons potentiate virus-induced apoptosis through activation of the FADD/caspase-8 death signaling pathway. J Virol 2000;74:1513–23.

51. Barnes BJ, Kellum MJ, Field AE, Pitha PM. Multiple regulatory domains of IRF-5 control activation, cellular localization, and induction of chemokines that mediate recruitment of T lymphocytes. Mol Cell Biol 2002;22:5721–40.

52. Cheng TF, Brzostek S, Ando O, et al. Differential activation of IFN regulatory factor (IRF)-3 and IRF-5 transcription factors during viral infection. J Immunol 2006;176:7462–70.

53. Du M, Beatty LG, Zhou W, et al. Insulator and silencer sequences in the imprinted region of human chromosome 11p15.5. Hum Mol Genet 2003;12:1927–39.

54. Ning S, Huye LE, Pagano JS. Regulation of the transcriptional activity of the IRF7 promoter by a pathway independent of interferon signaling. J Biol Chem 2005;280:12262–70.

55. Barnes BJ, Richards J, Mancl M, et al. Global and distinct targets of IRF-5 and IRF-7 during innate response to viral infection. J Biol Chem 2004;279:45194–207.

56. Alcorta DA, Xiong Y, Phelps D, et al. Involvement of the cyclin-dependent kinase inhibitor p16 (INK4a) in replicative senescence of normal human fibroblasts. Proc Natl Acad Sci U S A 1996;93:13742–7.

57. Rogan EM, Bryan TM, Hukku B, et al. Alterations in p53 and p16INK4 expression and telomere length during spontaneous immortalization of Li-Fraumeni syndrome fibroblasts. Mol Cell Biol 1995;15:4745–53.

58. Stein GH, Drullinger LF, Soulard A, Dulic V. Differential roles for cyclin-dependent kinase inhibitors p21 and p16 in the mechanisms of senescence and differentiation in human fibroblasts. Mol Cell Biol 1999;19:2109–17.

Molecular Cancer Research

Interferon Regulatory Factors IRF5 and IRF7 Inhibit Growth and Induce Senescence in Immortal Li-Fraumeni Fibroblasts

Qunfang Li, Lin Tang, Paul Christopher Roberts, et al.

Mol Cancer Res 2008;6:770-784.